Journal of Propulsion and Power
Vol. 23, No. 1, January–Febrary 2007

Technical Notes

TECHNICAL NOTES are short manuscripts describing new developments or important results of a preliminary nature. These Notes should not exceed 2500 words (where a figure or table counts as 200 words). Following informal review by the Editors, they may be published within a few months of the date of receipt. Style requirements are the same as for regular contributions (see inside back cover).

Performance Analysis of an Infinite Array Linear Clustered Plug Nozzle

Marco Geron,* Renato Paciorri,† Francesco Nasuti,‡ and Filippo Sabetta§
University of Rome "La Sapienza," Rome 00184, Italy

DOI: 10.2514/1.20094

Introduction

IN the challenge of realizing a new generation of space launchers, either single or two stage to orbit, an important role is played by the performance of the engine expansion system working in a varying pressure environment. In this framework a great interest has been devoted to the linear plug nozzle, which has been the subject of several studies in the last decade [1–6]. The plug nozzle is an external-expansion nozzle that yields self-adaptation of the exhaust jet to varying ambient pressure ratios, in a certain range of the launcher trajectory. This self-adapting capability allows high nozzle expansion ratios while avoiding the risks of flow separation that would exist in equivalent bell nozzles. The plug nozzle is made of a primary internal expansion nozzle, which is a conventional supersonic nozzle, and an external-expansion ramp, referred to as the plug surface. Most of the different engineering solutions proposed for plug nozzles have the following common feature: the primary expansion is made through a cluster of bell nozzles (or modules) exhausting onto a common linear plug surface [7–9].

The primary nozzle partitioning allows easier manufacturing, lower thermal loads, easier cooling and higher thrust vector capability. However, clustering causes additional performance losses due to three-dimensional flow inside the modules and to the interaction of jets exhausting from adjacent modules. For these reasons the three-dimensional features have to be studied in depth to better predict the engine performance and the expected mechanical and thermal loads for nominal operating conditions both at sea level and altitude and for differentially throttled modules as well. In fact, the thrust vectoring could be achieved by differential throttling of modules and, when thrust requirement is reduced in the final part of the ascent, some of the modules could be intentionally shut down.

To this goal, the present paper studies by numerical simulation, the three-dimensional flow field generated by the modules on a reference linear plug surface. The attention is focused on the effects of the three-dimensional flow features that take place when two different kind of modules are considered: the first module is obtained by dividing the reference two-dimensional primary nozzle by vertical walls and the second one is a full three-dimensional round-to-square nozzle. The performance analysis of these different module configurations allows weighing separately the role of clustering (i.e., just divide the primary nozzle into modules with infinitely thin flat walls) and the role of module design. A further subject of this study is the analysis of the effects produced by the shut down of a module of the cluster, for both module configurations. The analysis of the different configurations is made by comparing the thrust losses with the reference two-dimensional solution.

Test Case Description

All simulations consider a plug nozzle formed by a cluster of modules, with a square exit cross section, which discharge their supersonic jets over a single linear plug surface (see Fig. 1). The two-dimensional method of characteristics is used to design the linear plug surface in order to avoid the reflection of the waves coming from the module corner. The area ratio of the modules is 3.25, so that the isentropic exit Mach number is $M = 2.72$. Each module forms an angle $\theta = 24$ deg with the horizontal plane. The design pressure ratio of the overall plug nozzle is $PR = p_c/p_a = 200$, where p_c indicates chamber pressure and p_a indicates ambient pressure. The jet discharges in an ambient where the air is at rest. For the sake of simplicity, the gas of the external ambient and of the nozzle jets is assumed to be inert air.

The modules are designed with two different geometries. The first one (Rec module) is a two-dimensional truncated ideal nozzle [10] having constant width and rectangular cross section. The second one (R2S module [11]) is more complex. Indeed, the module area varies according to the design of an axisymmetric truncated ideal nozzle. Nevertheless, only the first part of the module, including the whole converging section and half of the diverging section, has a circular cross section. In the second half of the diverging section the area continues to follow the axisymmetric area law but the cross section gradually changes its shape. From the midpoint of the diverging section to its exit the module transforms from a circle to a square. The transformation law of the section shape is obtained by a linear combination. Specifically, if x, x_c, and x_s denote, respectively, the vectors containing the boundary nodes of the transformed section, of the unit area circular section and of the unit area square section, the transformation law is given by

$$x = x_s\alpha + \mathrm{x}_c(1-\alpha) \tag{1}$$

where α is a parameter linearly varying with the section position, whose value is $\alpha = 0$ at midpoint of the diverging section and $\alpha = 1$ at module exit. Since the section shape is given by Eq. (1), the section is scaled in order to obtain the area predicted by the axisymmetric nozzle law.

These two different geometries for the modules were selected because they represent the configurations used both in the study and in the design of the clustered plug nozzles. The selection of modules with a square exit section was made according to [11]. The reason is that the square shape yields the minimum module thrust loss among

---

Presented as Paper 4910 at the 39th AIAA/ASME/SAE/ASEE Joint Propulsion Conference and Exhibit, Huntsville, Alabama, 20–23 July 2003; received 19 September 2005; revision received 25 May 2006; accepted for publication 25 May 2006.

*Ph.D., Department of Mechanics and Aeronautics, Via Eudossiana 18.
†Professor, Department of Mechanics and Aeronautics, Via Eudossiana 18.
‡Professor, Department of Mechanics and Aeronautics, Via Eudossiana 18. Senior Member AIAA.
§Full Professor, Department of Mechanics and Aeronautics, Via Eudossiana 18.

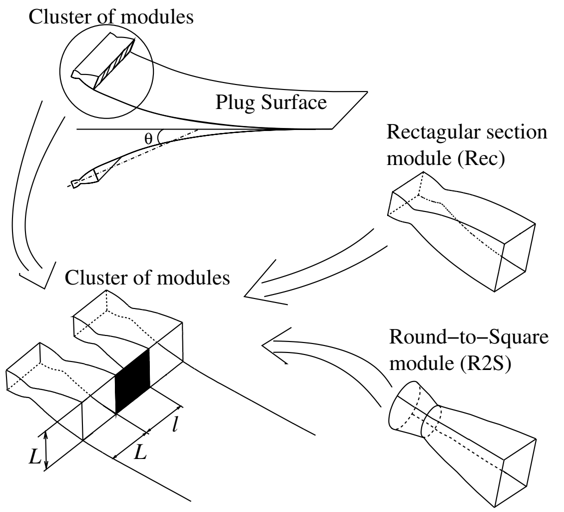

Fig. 1 Test case configurations.

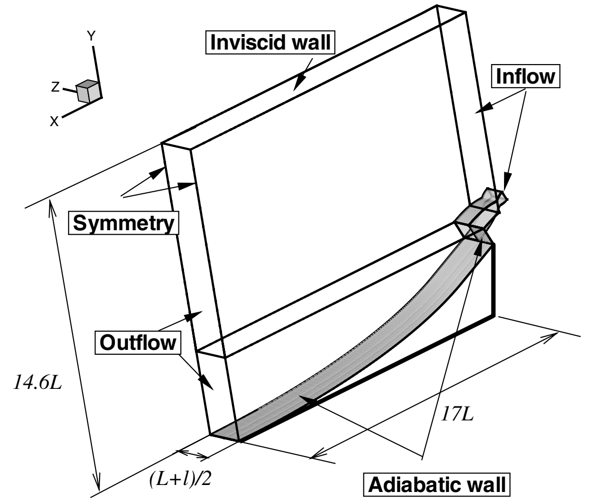

Fig. 2 Computational domain and boundary conditions.

the possible rectangular shapes, which avoid the losses generated by circular cross-section modules. The latter losses are caused by the low pressure regions between adjacent modules (see [7]).

The test cases differ not only for the geometry of the modules but also for their arrangement. Two configurations are considered: in the first case, the modules are arranged so that the gap between two adjacent modules is of zero width, in the second case the gap size is equal to the width of the nozzle exit. The latter case reproduces the situation caused by turning off a module. This can occur for an accidental failure of the engine but it can also be caused intentionally to reduce thrust.

Table 1 summarizes the main characteristics and the operating conditions of each test case analyzed in this paper.

Flow Modeling and Numerical Method

The flow is modeled using the Reynolds averaged Navier–Stokes equations for a compressible perfect gas and the Spalart–Allmaras turbulence model [12]. This turbulence model was chosen because it is strictly "local," in the sense that the coefficients in the equations depend only on quantities that can be computed from the distance to the nearest wall and from the velocity field and its first order tensor in each point. This property is important when, as in the present cases, geometrical configurations include more than a single wall. In addition, the Spalart–Allmaras model has shown good performance in the computation both of compressible flows [13–15] and of complex three-dimensional flows [16,17].

Numerical simulations analyzed in this paper are performed using a gasdynamics solver developed by the authors. The solver is based on a Godunov finite volume method [18] and the numerical scheme is second order accurate in space and time. The solution is advanced in time by means of an explicit predictor-corrector integration. Local time step is used to speed up convergence to steady state.

Because of the existence of symmetry planes, the computational domain considers only half of a module and half of a gap between two active modules and a strip of plug bounded by the symmetry planes of the module and of the gap (see Fig. 2). These symmetry planes in the z direction result in a domain representing an "infinite array" of modules in the z direction. The computational domain includes a tall region above the module and the plug in order to simulate flow conditions as similar as possible to the air at rest.

The boundary conditions enforced in the computational domain are reported in Fig. 2. As regards to the inflow conditions, some remarks are necessary. At the inlet section of the modules the chamber total temperature and total pressure are enforced, whereas at

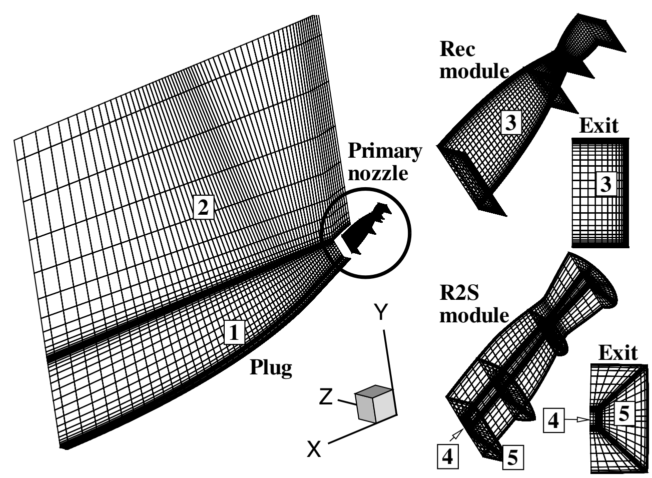

Fig. 3 Computational meshes.

Table 1 Test case definition

Test case	Rec-0	Rec-1	R2S-0	R2S-1
Chamber temperature, K	750	750	750	750
Chamber pressure, MPa	0.818	0.818	0.818	0.818
L, cm	22	22	22	22
PR	200	200	200	200
Primary module	Rec	Rec	R2S	R2S
Gap (l/L)	0	1	0	1
Wall	Adiabatic	Adiabatic	Adiabatic	Adiabatic

Table 2 Number of cells for each block

Region	Block	Coarse	Fine
Plug	1	$60 \times 40 \times 20$	$120 \times 80 \times 40$
	1 mod.	$60 \times 40 \times 40$	$120 \times 80 \times 80$
	2	$70 \times 20 \times 20$	$140 \times 40 \times 40$
	2 mod.	$70 \times 20 \times 40$	$140 \times 40 \times 80$
Rec nozzle	3	$45 \times 40 \times 20$	$90 \times 80 \times 40$
R2S nozzle	4	$32 \times 20 \times 10$	$64 \times 40 \times 20$
	5	$32 \times 40 \times 22$	$64 \times 80 \times 44$

Table 3 Total number of cells for each test case

Test case	Coarse	Fine
Rec-0	112,000	896,000
Rec-1	188,000	1,504,000
R2S-0	110,560	884,480
R2S-1	186,560	1,492,480

Table 4 Thrust coefficient contributions due to the different parts of plug nozzle

Test case	Module	Plug	Total	Efficiency (%)
Rec-0	$1.3507 \pm (0.0034)$	$0.2116 \pm (0.0007)$	$1.5623 \pm (0.0041)$	97.65
R2S-0	$1.3411 \pm (0.0036)$	$0.2015 \pm (0.0003)$	$1.5427 \pm (0.0039)$	96.42
Rec-1	$1.3507 \pm (0.0034)$	$0.1573 \pm (0.0020)$	$1.5080 \pm (0.0053)$	94.26
R2S-1	$1.3411 \pm (0.0036)$	$0.1556 \pm (0.0038)$	$1.4968 \pm (0.0074)$	93.56
2-D	$1.3588 \pm (0.0008)$	$0.2107 \pm (0.0002)$	$1.5695 \pm (0.0011)$	98.10
Ideal	1.3807	0.2193	1.5999	100.00

the outside inflow section the total temperature and total pressure enforced are slightly greater than the ambient values in order to obtain a low speed stream outside the nozzle exhaust jet. This kind of boundary condition allows overcoming the numerical difficulties in simulating air at rest, without introducing significant differences with respect to a truly quiescent gas.

Numerical simulations have been carried out on meshes characterized by different structured blocks of cells (see Fig. 3). In the test cases where the ratio l/L is zero (Rec-0 and R2S-0), block 1 discretizes the region bounded by the plug surface and block 2 is used for upper region. When a gap between the modules is present (Rec-1 and R2S-1), blocks 1 and 2 are modified increasing the dimension and number of cells in z direction. The modules are discretized by two different meshes: the rectangular section nozzle is discretized by a single block (block 3) whereas two blocks (blocks 4 and 5) are used for the R2S nozzle. In particular, block 4 is placed along the nozzle axis and its crosswise sections have always a square shape; the block 5 is a "C" block surrounding block 4.

To assess the grid convergence of solutions, each test case was computed on two meshes with increasing level of refinement. The coarse meshes are obtained from the fine ones deleting one node out of two in each coordinate direction. Tables 2 and 3 report the number of cells of each block and the total number of cells for each test case and discretization level.

Performance Analysis

To analyze the effects of module shape and of module shutdown on the overall nozzle performance, the efficiency of the different nozzles is analyzed by comparison of their vacuum thrust coefficients (C_F). The nozzle thrust coefficient is defined as the ratio of thrust to a reference thrust value. This reference value is obtained as the product of chamber pressure (p_c) and the throat area (A_t) available to exhaust gas [note that this product is equivalent to the product of nozzle mass flow rate ($\dot{m}$) and characteristic velocity (c^*)]. Each nozzle thrust coefficient is compared with the ideal value obtained by ideal isentropic expansion to the nozzle design pressure ratio and to the value obtained by a two-dimensional (no-module) viscous simulation. For a better comparison, thrust (and thus thrust coefficient) is split into the module contribution and the plug contribution (see Table 4). Each value is followed by its grid convergence index (GCI) reported in brackets. This index, proposed by Roache [19], provides an error bandwidth for the numerical predictions and requires the computation of numerical solutions on at least two discretization levels. It is worth observing that the GCI of the total C_F predictions is at most 0.5% of the predicted value.

The comparison of the 2-D with the ideal C_F shows a 1.9% reduction. Two kind of losses lead to the above thrust reduction. The first one is the thrust loss due to friction on primary nozzle and plug walls. The second one is due to primary nozzle divergence loss which would be zero only for an ideal primary nozzle with uniform flow at the nozzle exit. This is not the present case where a truncated ideal contour nozzle is considered. The splitting of thrust contributions emphasizes the role of primary nozzle, as the internal expansion provides most of the thrust (86%) whereas the plug surface provides the remaining 14%.

Partitioning of the primary nozzle using the Rec modules adds the side wall friction. The sidewall friction reduces performance of an additional 0.5% (2.4% reduction relative to ideal).

The use of R2S modules further penalizes the thrust coefficient. The total reduction of module contribution has been calculated in the present test case as 0.7% (comparing the module contribution of the test cases R2S-0 and Rec-0). Although this value is obviously a function of module geometry and of the considered area ratio, it is of the same order of magnitude of that found in [11]. The flow field at exit of the R2S module is characterized by higher nonuniformity than the Rec module exit. These gradients at the module exit yield an effect also on the plug contribution to thrust. Therefore, the total loss due to R2S shape increases from the 0.7% value of the module to the overall 1.3%. These results show that care should be devoted to the design of module shape as a more accurate design could allow recovering part of the above loss.

Turning off modules obviously does not contribute to module efficiency, however, the existence of large areas of plug surface unfilled with high pressure module exhaust gas yields a large efficiency reduction. In particular, the presence of a gap as large as the module reduces the plug surface contribution of C_F by about one quarter meaning a total efficiency reduction of about 3%. The flow nonuniformities at module exit have a marginal role on plug C_F in this case, because of the prevailing role of losses due to the sudden side expansion needed to fill the gap between modules. The large gap, therefore, reduces the performance difference between the R2S and Rec cases. Indeed, the R2S-1 total C_F is only 0.7% less than Rec-1 and this value coincides with difference between the module contribution. In practice, when a large gap is present, the plug contribution is weakly affected by the module shape.

Conclusions

The analysis of the test cases studied in this work and the comparison with the two-dimensional results has allowed us to quantify the three-dimensional flow effects due to module configuration on the performance for a linear clustered plug nozzle. The module shape is a critical element for the nozzle performance. Specifically, the partitioning of the primary nozzle with round-to-square modules causes a vacuum thrust reduction with respect to the two-dimensional model which can exceed 1%. In the operating conditions characterized by turned off modules the performance loss is larger but the differences due to the module shape are smaller and mostly due to module contribution.

These results show the kind of performance improvement that can be obtained focusing the efforts in the module design. The goal of the design should be to reduce the module exit flow nonuniformity which is the main cause of both module and plug losses.

References

[1] Nasuti, F., and Onofri, M., "Methodology to Solve Flowfields of Plug Nozzles for Future Launchers," *Journal of Propulsion and Power*, Vol. 14, No. 3, 1998, pp. 318–326; see also AIAA Paper 97-2941, 1997.

[2] Ruf, J. H., and McConnaughey, P., "A Numerical Analysis of Three-Dimensional Aerospike," AIAA Paper 97-3217, July 1997.

[3] Hagemann, G., Immich, H., and Dumnov, G., "Critical Assessment of the Linear Plug Nozzle Concept," AIAA Paper 2001-3683, July 2001.

[4] Immich, H., Nasuti, F., Onofri, M., and Caporicci, M., "Experimental and Numerical Analysis of Linear Plug Nozzles," AIAA Paper 98-1603, Apr. 1998.

[5] Fick, M., and Schmucker, R., "Linear Aerospike Engine Performance Evaluation," AIAA Paper 97-3305, July 1997.

[6] Immich, H., and Caporicci, M., "Status of the FESTIP Rocket Propulsion Technology Programme," AIAA Paper 97-3311, 1997.

[7] Nasuti, F., and Onofri, M., "Theoretical Analysis and Engineering Modeling of Flowfields in Clustered Module Plug Nozzles," *Journal of Propulsion and Power*, Vol. 15, No. 4, 1999, pp. 544–551.
[8] Wang, T.-S., Droege, A., D'Agostino, M., Lee, Y.-C., and Williams, R., "Asymmetric Base: Bleed Effect on Aerospike Plume-Induced Base-Heating Environment," *Journal of Propulsion and Power*, Vol. 20, No. 3, 2004, pp. 385–393.
[9] Fick, M., and Schmucker, R., "Performance Aspect of Plug Cluster Nozzles," *Journal of Spacecraft and Rockets*, Vol. 33, No. 4, 1996, pp. 507–512.
[10] Ahlberg, J. H., Hamilton, S., Migdal, D., and Nilson, E. N., "Truncated Perfect Nozzles in Optimum Nozzle Design," *ARS Journal*, Vol. 31, No. 5, 1961, pp. 614–620.
[11] Nguyen, T., Spencer, R., and Siebenhaar, A., "Aerodynamic Performance of Round-to-Square Nozzle," *Proceedings of the 35th Heat Transfer and Fluid Mechanics Institute*, Dept. of Mechanical Engineering, California State Univ., Sacramento, 1997.
[12] Spalart, P. R., and Allmaras, S. R., "A One-Equation Turbulence Model for Aerodynamic Flow," *La Recherche Aerospatiale: Bulletin Bimestriel de l'Office National d'Etudes et de Recherches Aerospatiales*, No. 1, 1994, pp. 5–21.
[13] Paciorri, R., Nasuti, F., and Sabetta, F., "Evaluation of Turbulence Modeling in Supersonic Afterbody Computations," AIAA Paper 2001-3039, June 2001.
[14] Paciorri, R., Dieudonné, W., Degrez, G., Charbonnier, J.-M., and Deconinck, H., "Exploring the Validity of the Spalart-Allmaras Turbulence Model for Hypersonic Flows," *Journal of Spacecraft and Rockets*, Vol. 35, No. 2, 1998, pp. 121–126.
[15] Nasuti, F., and Onofri, M., "Analysis of In-Flight Behavior of Truncated Plug Nozzles," *Journal of Propulsion and Power*, Vol. 17, No. 4, Jul.–Aug. 2001, pp. 809–817.
[16] Paciorri, R., Di Mascio, A., and Favini, B., "A Comparative Study of Turbulence Models for Junction Flow," AIAA Paper 2002-2964, June 2002.
[17] Paciorri, R., Bonfiglioli, A., Di Mascio, A., and Favini, B., "RANS Simulations of a Junction Flow," *International Journal of Computational Fluid Dynamics*, Vol. 19, No. 2, 2005, pp. 179–189.
[18] Di Mascio, A., and Favini, B., "A Two-Step Godunov-Type Scheme for the Euler Equation," *Meccanica*, Vol. 26, No. 2–3, 1991, pp. 179–188.
[19] Roache, P. J., "Quantification of Uncertainty in Computational Fluid Dynamics," *Annual Review of Fluid Mechanics*, Vol. 29, Jan. 1997, pp. 123–160.

T. Wang
Associate Editor